PHYSICAL REVIEW A VOLUME 36, NUMBER 3 AUGUST 1, 1987

Noise-induced bistability at the T-I–T-II transition in superfluid He II

D. Griswold and J. T. Tough
Department of Physics, The Ohio State University, Columbus, Ohio 43210-1106
(Received 28 January 1987)

We present preliminary experiments which indicate a dramatic effect of external noise on superfluid turbulence in thermal counterflow. This turbulent system is in many ways ideal for the study of noise-driven nonlinear dynamical systems. It contains a well-defined continuous transition (the T-I–T-II transition), and noise can be easily imposed on the driving heat current. Previous work has shown that the superfluid turbulence system is described by a single nonlinear amplitude equation, and it can be expected to show some of the rich noise-induced behavior found in theoretical treatments of such systems. We find that external noise dramatically modifies the T-I–T-II transition and induces bistability.

Several years ago Horsthemke and Lefever[1] made the rather remarkable proposal that there exists a new set of phenomena within the class of phase transitions. The ideas of equilibrium phase transitions have been extended over the last decade to include transition phenomena encountered in nonequilibrium systems.[2] What Horsthemke and Lefever suggested was that the concept of phase transition can be extended even further, to a fundamentally new set of transition phenomena which occur only in nonequilibrium systems coupled to a randomly fluctuating environment. Not only are such transitions new and fascinating objects of study, but they are surprisingly nonintuitive. In a wide range of systems it is found that the influence of environmental noise *stabilizes* the system, or postpones the transition to a larger (average) value of the control parameter. The noise can also generate bifurcations not present in the deterministic environment.

While it may be argued on technical grounds that the extension of phase-transition concepts to these noise-driven transitions is unjustified,[3] the significance of these phenomena is not reduced. It is clear that the effects of parametric modulation or noise on nonlinear dynamical systems are dramatic, and the understanding of these effects is an important fundamental problem. One might expect that the effects of environmental noise would be rather trivial: The system will simply "average out" the fluctuations, and the output will simply be spread about the deterministic state. Theoretical studies[1] of simple nonlinear systems show that these intuitive expectations are oversimplified and a much richer variety of behaviors is induced by the noise than is possible under strictly deterministic conditions. The interplay between the nonequilibrium of the system and the randomness of the environment leads to drastic changes in the macroscopic states.[4]

Noise-induced effects have been predicted for a wide range of nonlinear dynamical systems. Generally these are assumed to be spatially homogeneous or "zero dimensional," and described by a single intensive variable (such as a mode amplitude). The coupling of the system to the environment is described on this phenomenological level by a control parameter λ. Several different theoretical approaches have been taken to determine the effect of noise in the parameter λ to the time-averaged behavior of the system.[1,5,6] Often the noise is assumed to be "white," linear, and Gaussian. The influence of finite correlation time ("colored noise"[7]) and quadratic effects[7–9] have been studied in various theoretical models.

There are only a few physical systems in which noise-induced phenomena have actually been observed. Smythe, Moss, and McClintock[10] have pioneered the use of analog simulators to explore the influence of noise on particular differential equations. Robinson, Moss, and McClintock[11] have recently applied these techniques to a study of stochastic postponements in a bistable system, and find good agreement with the predictions of Welland and Moss[12] based upon the theoretical approach of Horsthemke and Lefever. In the area of classical hydrodynamics, Donnelly, Reif, and Suhl,[13] Ahlers, Hohenberg, and Lücke,[14] and Gollub and Benson[15] have explored the effects of simple monochromatic modulation of the control parameter. Electrohydrodynamic instabilities in liquid crystals have been an important experimental area for noise-induced effects. Recently, Brand, Kai, and Wakabayashi[16] have demonstrated that not only can the transition to turbulence in these systems be postponed by noise, but the bifurcation sequence can be altered as well.

In this paper we give the results of a preliminary study of the effects of noise on superfluid turbulence (SFT).[17] Moss and Welland[18] first suggested the use of the SFT system to study noise-driven phenomena and applied the methods of Horsthemke and Lefever[1] to the dynamical equation proposed by Vinen.[19] Although this equation is now believed to be an oversimplified description of the SFT system, the results of the present experiments largely vindicate the basic ideas proposed by Moss and Welland. On the microscopic level SFT is understood as a tangle of quantized vortex lines,[19] and the macroscopic properties of the homogeneous SFT state have been reproduced in computer simulations of the vortex tangle.[20] At the macroscopic level, the transition to the homogeneous state (the T-I–T-II transition in liquid He II) has been success-

fully described by a phenomenological amplitude equation[21] and appears to be characterized by a single amplitude, the vortex line density L. From an experimental viewpoint the SFT system is also an excellent candidate for the study of noise-induced effects since the noise is easily added to the drive parameter, the fluctuating output can be detected, and the time constants of the system are well understood.[22]

We produce and detect the superfluid turbulence using a thermal counterflow apparatus. This SFT is a special case of that produced in more general flows with both heat and mass transport. Thermal counterflow has the advantage of being experimentally easy to produce and extensively studied. The apparatus is shown schematically in Fig. 1, and described in detail previously.[23] The glass flow tude is 1 cm long (l) and 132 μm in diameter (d). It connects a small cell containing a heater with a large reservoir of helium maintained at a temperature of 1.75 K. A heat current $\dot{Q}$ in the tube of cross-sectional area A generates a counterflow of the superfluid and normal fluid components at a relative speed V where

$$V=\dot{Q}/A\rho_p ST \ . \tag{1}$$

Here ρ_s is the superfluid density and S the entropy density of the helium at temperature T. If V is sufficiently large, a superfluid turbulent state is present in the flow tube and is characterized by a steady-state vortex line density (length of line per unit volume) L_0. The "friction" between the vortex lines and the normal fluid flow is the source of a chemical potential difference $\Delta\mu$ between the cell and the reservoir. If the SFT is homogeneous,[24] then it can be shown that $\Delta\mu$ ir related to L_0 as

$$\Delta\mu=(lB\rho_n\kappa/3\rho)L_0V \ , \tag{2}$$

where ρ_n is the normal fluid density, ρ the total density, κ the quantum of circulation, and B a parameter representing the strength of the normal fluid-vortex line interaction.[25] In our apparatus, the chemical potential difference $\Delta\mu$ is transduced into a pressure difference and detected with a capacitive pressure transducer as discussed previously.[23] Figure 2 shows the output of the capacitance bridge as a function of the heat current $\dot{Q}$. The kink in these data near 120 μW signals a transition in the SFT from a state T-I to state T-II.[17] Figure 3 shows the characteristic "phase diagram" for this transition, obtained from the data in Fig. 2 using Eq. (2) to calculate the vortex line density L_0. The right-hand scale gives the vortex line density in a convenient dimensionless form. The solid line in Fig. 2 is the result of the computer simulation of Schwarz[20] for homogeneous SFT.

The underlying physics of the T-I–T-II transition remains obscure, as does the nature of the T-I state itself. A phenomenological description of the transition has recently been given by Horsthemke and Schumaker.[21] They have been able to identify the form of the underlying bifurication from an analysis of the *intrinsic* noise observed at the transition.[22,23] Assuming that the SFT can be described by a single amplitude, they show that the normal form of the imperfect pitchfork bifurcation, with noise, provides a very satisfactory model in the neighborhood of the T-I–T-II transition. The imperfect pitchfork bifurcation that Horsthemke and Schumaker identify with the T-I–T-II transition is an example of the lowest codimension bifurcation that can mediate continuous transitions between steady states. Their model gives a unified description of the steady-state line density (Fig. 3), the relaxation time, and the intrinsic noise, in agreement with experimental observations. One of the parameters that must be chosen to fit the data is the "paracritical point," $\dot{Q}_c=121$ μW. In Fig. 2 we have plotted the reduced heat current

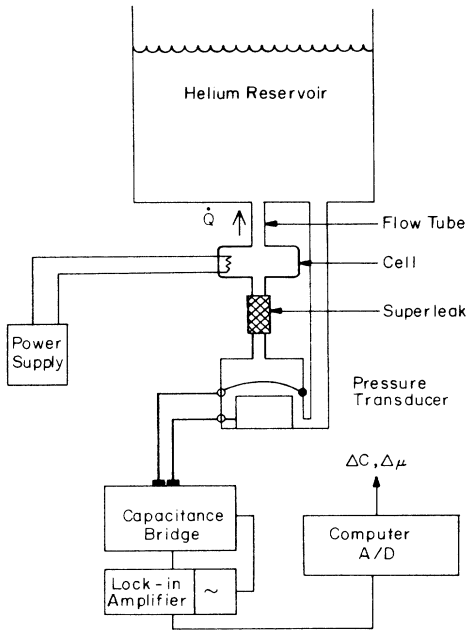

FIG. 1. Schematic diagram of the apparatus used to produce and detect the superfluid turbulence.

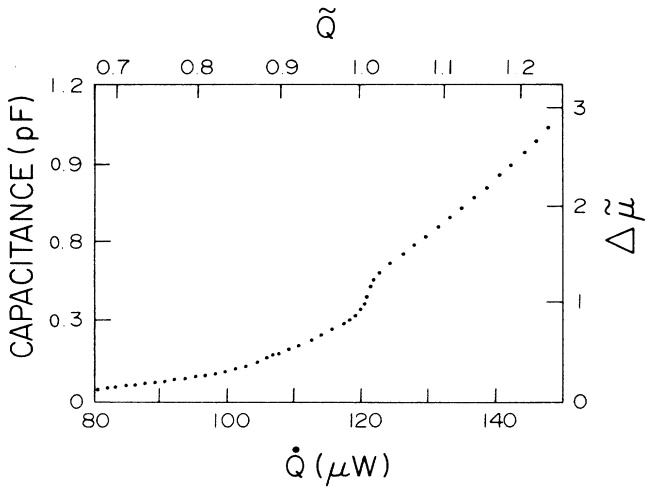

FIG. 2. Output of the capacitance bridge as a function of the heat current $\dot{Q}$. The capacitance is proportional to the chemical difference produced by the superfluid turbulence. The reduced chemical-potential difference $\Delta\tilde{\mu}$ [Eq. (4)] is shown on the right-hand scale and the reduced heat current $\tilde{Q}$ [Eq. (3)] is shown on the upper scale. The kink in the data near 120 μW signals the T-I–T-II transition.

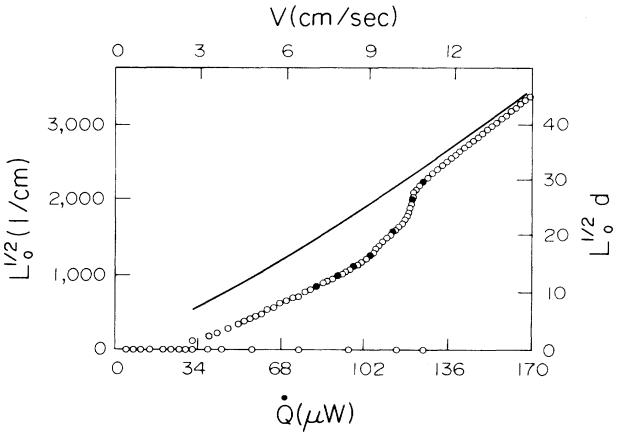

FIG. 3. Square root of the steady-state vortex line density L_0 as a function of the heat current $\dot{Q}$. The line density is obtained from the chemical-potential difference using Eq. (2). The upper scale gives the relative velocity of the superfluid and normal fluid [Eq. (1)]. The right-hand scale gives the line density in dimensionless form. The states T-I and T-II are labeled. The solid line is the result of a computer simulation of the vortex line density in homogeneous superfluid turbulence (Ref. 20).

$$\tilde{Q}=\dot{Q}/\dot{Q}_c \tag{3}$$

on the upper scale and the reduced chemical-potential difference

$$\Delta\tilde{\mu}=\Delta\mu(\dot{Q})/\Delta\mu(\dot{Q}_c) \tag{4}$$

on the right-hand scale. These reduced variables will be useful for discussing the influence of external noise on the T-I–T-II transition.

Consider a nonlinear dynamical system, described by the single amplitude x, and satisfying the equation

$$\dot{x}=f(x,\lambda)\ , \tag{5}$$

where λ is the control parameter. The stationary states of this system are given by the function $x_0(\lambda)$ which is a solution to the equation $f(x,\lambda)=0$. If the control parameter consists of a steady part λ_0 and a noisy part $\delta\lambda$, then the amplitude x is noisy, and the steady state of the system is described by the stationary probability $p(x)$. Horsthemke and Lefever[1] have shown that macroscopic steady states are associated with the extrema of $p(x)$. Those values x_m for which $p(x)$ is a maximum give the "most probable states" and can be associated with the "phases" of the system. In general the stochastic steady state $x_m(\lambda)$ is different from the deterministic steady state $x_0(\lambda)$.

In order to add noise to the drive parameter of the SFT system, it is only necessary to add noise to the heat current $\dot{Q}$. Figure 4 shows a schematic drawing of the apparatus used. The output of a white-noise source[26] is sent through a Butterworth filter to one input of a summing amplifier. An example of the Gaussian distribution of this signal is given in Fig. 5. The dc component of the noise source is zeroed and the output V_0 from a dc power supply is added to the noise in the summing amplifier and sent to the cell heater of resistance R. The voltage across

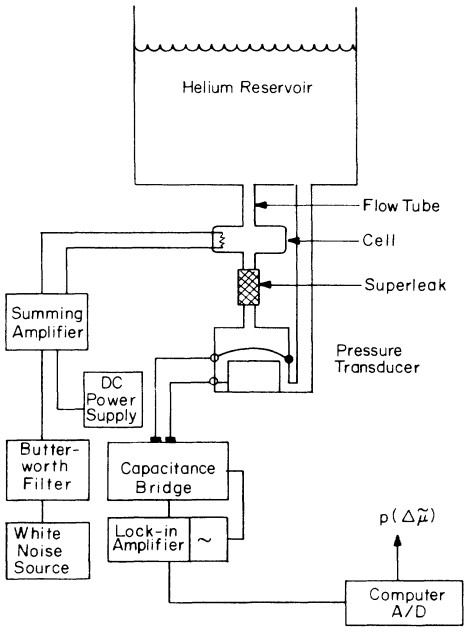

FIG. 4. Schematic diagram of the apparatus used to add noise to the heat current and detect the fluctuating chemical-potential difference.

the heater is then

$$V_h=V_0+\delta V\ , \tag{6}$$

where δV is Gaussian noise of zero mean, and variance[27] σ_v. The heat current driving the SFT can then be written as

$$\dot{Q}_h=\dot{Q}+\delta\dot{Q}\ , \tag{7}$$

where $\delta\dot{Q}$ is now non-Gaussian noise (it is sharper than Gaussian) of rms amplitude $\sigma^2=\sigma_y^2/R$, and the steady heat current is

$$\dot{Q}=(V_0^2+\sigma_v^2)/R\ . \tag{8}$$

A careful calibration of the steady heating produced by the noise source was carried out at 4.2 K (where the

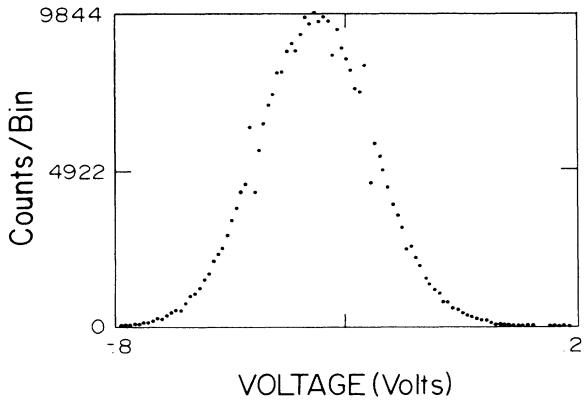

FIG. 5. Output of the noise source.

liquid helium is "normal") to ensure that there were no contributions other than (σ_v^2/R) such as eddy current heating.[28]

Because of the rather long thermal relaxation time of the system, any high-frequency noise components will be attenuated and will not contribute to uniform fluctuations of the drive parameter. Therefore the noise generator output is sent through a low pass filter (Fig. 4) set at 5.0 Hz, making the noisy heat current $\delta\dot{Q}$ "colored."

When the external noise is imposed on the heat current, the chemical potential difference across the flow tube (Fig. 2) fluctuates about some mean value. We analyze these fluctuations by producing a probability density $p(\Delta\mu)$. Time-series data from the capacitance bridge circuit are processed by dividing equally the range of allowed output voltages into 100 bins. A voltage falling in the range of a given bin increments a counter associated with that bin. The probability density can then be obtained as a plot of the number of counts in a bin as a function of bin number. Such a plot represents about 50 000 data points. Converting voltages to equivalent capacitances, or relative chemical-potential differences (see Fig. 2), the bins can be labeled with $\Delta\tilde{\mu}$.

Our experimental procedure is to fix the noise amplitude σ^2 and obtain probability densities $p(\Delta\tilde{\mu})$ for different values of the steady heat current $\dot{Q}$. From the maxima in each probability density we determine $\Delta\tilde{\mu}_m$, and use Eq. (2) to compute the corresponding vortex line density L_m. As discussed above, L_m is the most probable state of the SFT and equivalent to the state L_0 in the deterministic steady state. Using the values of L_m obtained in this manner, we can produce the phase diagram for the noise-driven SFT system analogous to Fig. 3 for the deterministic case.

In order to test the above analysis we first carried out the experimental procedure outlined above for a very low level of external noise. In this case we do not expect very profound noise-induced effects. The results shown in Figs. 6 and 7 are typical of many such data obtained using a noise amplitude σ^2 of about[29] 0.4 μW. Defining a relative amplitude as

$$\tilde{\sigma}^2=\sigma^2/\dot{Q}_c \ , \tag{9}$$

these results correspond to $\tilde{\sigma}^2=0.33\%$. Figure 6 shows nearly Gaussian and very narrow probability densities as would be expected from such weak noise. It should be noted that the *intrinsic noise*[23] from the SFT is very large near $\tilde{Q}=1$, and accounts for some of the width in the distributions shown in Fig. 6. Using the maxima in the probability densities to define $\Delta\tilde{\mu}_m$ and L_m as described above gives the phase diagram of Fig. 7. The dimensionless vortex line density $L_0^{1/2}d$ is shown as a function of the reduced heat current $\tilde{Q}$. The data from the noise-driven SFT are in excellent agreement with the deterministic vortex line density (Fig. 3) shown by the solid line. We conclude that the effect of low external noise is simply to cause the SFT system to fluctuate about its deterministic steady state.

The situation is quite different when large noise levels are used to drive the SFT. Figure 8 shows several examples of the probability densities obtained with $\tilde{\sigma}^2=49\%$

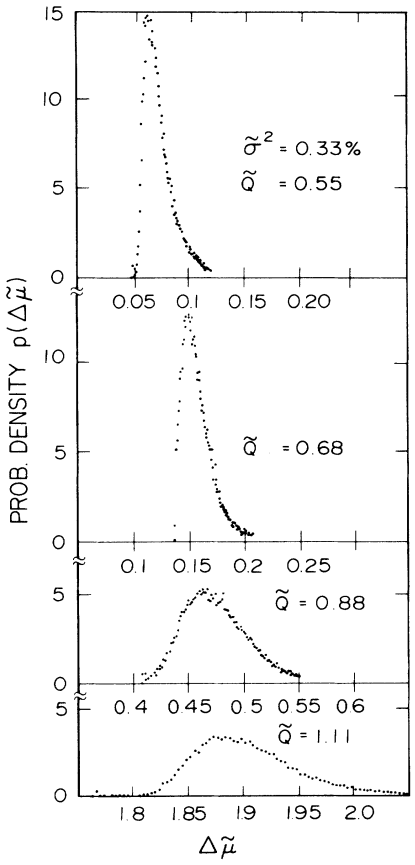

FIG. 6. Probability densities obtained with low-level noise ($\tilde{\sigma}^2=0.33\%$) at several different heat currents. Note that the zero on the $\Delta\tilde{\mu}$ axis is suppressed in order to display the narrow peaks at different values of $\Delta\tilde{\mu}$.

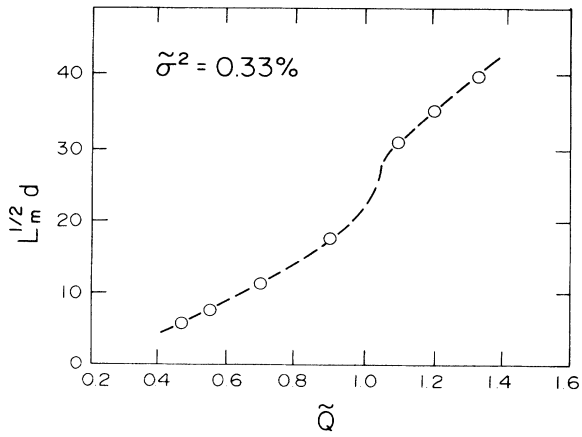

FIG. 7. The phase diagram for the superfluid turbulence with low-level noise. The open circles represent the vortex line densities L_m computed from the maxima in the probability densities (Fig. 6) using Eq. (2). The results agree well with the deterministic steady state (Fig. 3) shown by the dashed line.

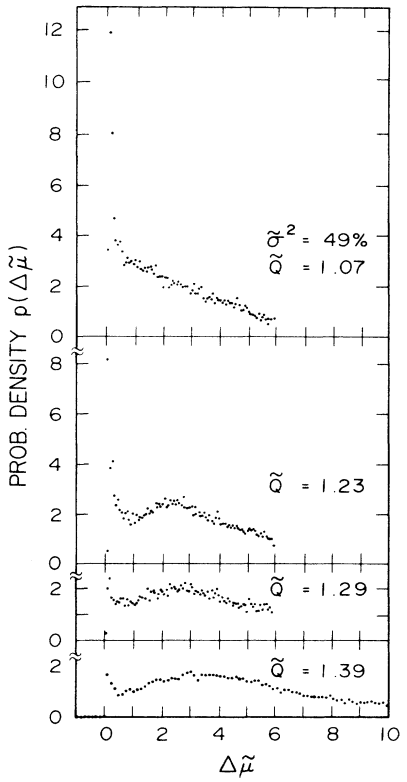

FIG. 8. Probability densities obtained with high-level noise ($\tilde{\sigma}^2=49\%$) at several different heat currents near the deterministic paracritical point ($\tilde{Q}=1$). At the larger values of $\tilde{Q}$ the densities become bimodal, although the lower narrow peak is not resolved at this resolution.

near the (deterministic) paracritical point $\tilde{Q}=1$. The data at large values of $\tilde{Q}$ show a very broad peak at values of $\Delta\tilde{\mu}_m$ which correspond to vortex line densities L_m quite close to the state T-II, and shown in Fig. 10. Not resolved in the data of Fig. 8 is a second peak in the density at very small values of $\Delta\tilde{\mu}$. Figure 9 gives an example of a probability distribution when this peak is resolved. This lower peak corresponds to the smaller values of the vortex line density shown in Fig. 10. Clear-

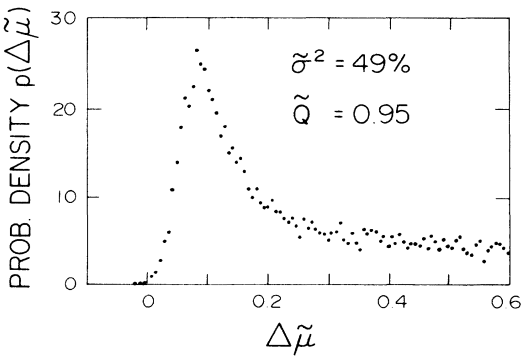

FIG. 9. Probability density obtained with high-level noise in which the narrow peak at low $\Delta\tilde{\mu}$ is resolved.

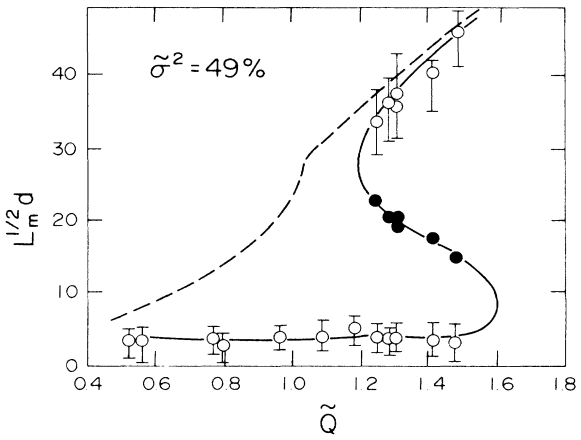

FIG. 10. The phase diagram for the superfluid turbulence with high-level noise. The open circles represent the vortex line densities L_m computed from the maxima in the probability densities (Figs. 8 and 9) using Eq. (2). The solid circles are obtained in a similar way from the minima in the probability densities and represent unstable states of the system. The solid line is simply a guide to the eye emphasizing the bisability induced by the noise. The dashed line is the deterministic steady state (Fig. 3).

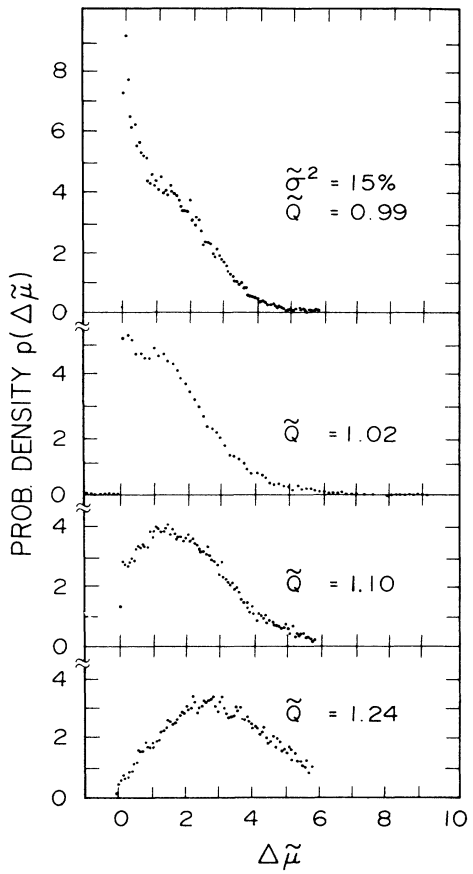

FIG. 11. Probability densities obtained with an intermediate-level noise ($\tilde{\sigma}^2=15\%$) at several different heat currents near the deterministic paracritical point. At the largest value of $\tilde{Q}$ there is no longer any evidence of the lower narrow peak.

ly over the range of $\tilde{Q}$ from 1.23 to 1.39 the stochastic phase diagram has become bistable. To emphasize this point we have also plotted the line densities corresponding to the *minima* in the probability densities (as closed circles) and have drawn the unstable branch of the phase diagram through the points. Such a construction is only justified if the SFT continues to be described by a single amplitude, but we have no evidence to the contrary.

The dramatic effect on the SFT phase diagram revealed in Fig. 10 is somewhat weakened when the noise amplitude is reduced. Figure 11 shows several examples of the probability densities obtained with $\tilde{\sigma}^2=15\%$, and Fig. 12 shows the corresponding phase diagram. The region of bistability is now much smaller than at $\tilde{\sigma}^2=49\%$, and the probability densities at large $\tilde{Q}$ are now monomodal. The probability density at $\tilde{Q}=1.02$ clearly shows the bimodal distribution for the bistable phase diagram.

It is interesting to note that the noise-induced bistability we have observed in SFT seems to be associated with a suppression of the T-I state. The T-II state is only slightly changed even with relatively large amounts of noise, while the T-I state is gradually "squeezed out." It is also significant that the T-I and T-II states can coexist, at least in a statistical sense, in the presence of noise. In this regard we also note that the time-series data for $\Delta\tilde{\mu}$ and the associated power spectra upper qualitatively the same both in and outside of the region of bistability.

Our experiments have revealed that SFT is an excellent system for the experimental study of noise-driven nonlinear dynamical systems as originally proposed by Moss and Welland. The deterministic states of the system are well characterized both in terms of phase diagram and time constants, and much of the microscopic physics is understood. Noise is easily applied to the drive parameter and the noise-induced effects are dramatic. We believe this is the first experimental demonstration of noise-induced bistability. Unfortunately, it is not a simple matter to compare these noise-induced effects with the phenomenological model of Schumaker and Horsthemke.[21] The noise is quadratic, colored, and large amplitude, all of which conspire to make the calculation difficult. Nevertheless, work is in progress, and results can be anticipated in the near future.

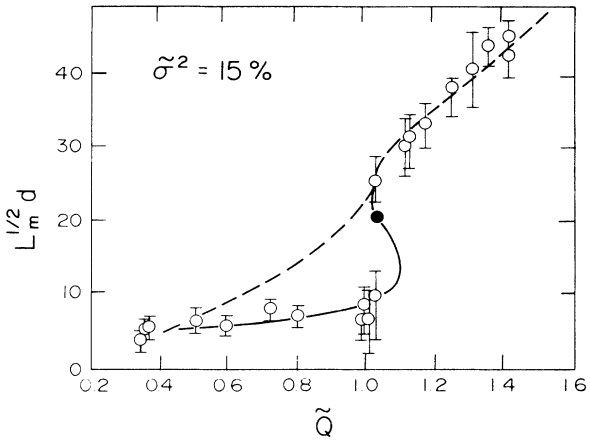

FIG. 12. The phase diagram for the superfluid turbulence with intermediate-level noise. The symbols are the same as in Fig. 10. The noise-induced bistability is much less pronounced compared with the high-level-noise results in Fig. 10.

The experiments also give some clues to the nature of the SFT states T-I and T-II. The homogeneous T-II state is extremely robust, and virtually unaffected by relatively large amounts of noise. On the contrary, the T-I state is drastically suppressed by external noise. Perhaps most puzzling of all is that the T-I and T-II states can coexist in the presence of noise. These observations should prove useful in determining the microscopic structure of the T-I state.

The authors are grateful to Professor W. Horsthemke and Professor Frank Moss for many useful discussions. This work has been supported by the National Science Foundation Low Temperature Physics Program, under Grant No. DMR-82-18052.

[1]W. Horsthemke and Lefever, *Noise-induced Transitions* (Springer-Verlag, Berlin, 1984).
[2]H. Haken, *Synergetics: An Introduction* (Springer-Verlag, Berlin, 1977).
[3]H. R. Brand, Phys. Rev. Lett. **54**, 605 (1985); F. Moss, P. V. E. McClintock, and W. Horsthemke, *ibid.* **54**, 606 (1985).
[4]For an excellent and very early discussion of this topic, see R. Landauer, Phys. Today **31** (No. 11), 23 (1978).
[5]M. Lucke and F. Schank, Phys. Rev. Lett. **54**, 1465 (1985).
[6]R. Graham and A. Schenzle, Phys. Rev. A **26**, 1676 (1982).
[7]M. San Miguel and J. M. Sancho, Z. Phys. B **43**, 361 (1981).
[8]W. Horsthemke, C. R. Doering, R. Lefever, and A. S. Chi, Phys. Rev. A **31**, 1123 (1985).
[9]H. Brand and A. Schenzle, J. Phys. Soc. Jpn. **48**, 1382 (1980).
[10]J. Smythe, F. Moss, and P. V. E. McClintock, Phys. Rev. Lett. **51**, 1062 (1983).
[11]S. D. Robinson, Frank Moss, and P. V. E. McClintock, J. Phys. A **18**, L89 (1985).
[12]G. V. Welland and Frank Moss, Phys. Lett. **89A**, 273 (1982).
[13]R. J. Donnelly, F. Reif, and H. Suhl, Phys. Rev. Lett. **9**, 363 (1962).
[14]G. Ahlers, P. Hohenberg, and M. Lücke, Phys. Lett. **53**, 48 (1984).
[15]J. P. Gollub and S. V. Benson, Phys. Rev. Lett. **41**, 948 (1978).
[16]H. R. Brand, S. Kai, and S. Wakabayashi, Phys. Rev. Lett. **54**, 555 (1985).
[17]For a general review of this system, see J. T. Tough, in *Progress in Low Temperature Physics,* edited by D. F. Brewer (North-Holland, Amsterdam, 1982), Vol. 8, Chap. 3.
[18]Frank Moss and G. V. Welland, Phys. Rev. A **25**, 3389 (1982).
[19]W. F. Vinen, Proc. R. Soc. London, Ser. A **242**, 493 (1957).
[20]K. W. Schwarz, Phys. Rev. Lett. **49**, 283 (1982).
[21]M. F. Schumaker and W. Horsthemke, Phys. Rev. A **36**, 354 (1987).
[22]C. P. Lorenson, D. Griswold, V. U. Nayak, and J. T. Tough, Phys. Rev. Lett. **55**, 1494 (1985).

[23]D. Griswold, C. P. Lorenson, and J. T. Tough, Phys. Rev. B **35**, 3149 (1987).

[24]If the turbulence is not homogeneous, then Eq. (2) is still a useful device for compressing the $\Delta\mu$ data. The line density in this case is then the "equivalent homogeneous density" in the sense of Ref. 18.

[25]There is some discrepancy regarding the appropriate values of B to be used in these calculations. C. E. Swanson, W. Wagner, C. Barenghi, and R. J. Donnelly, J. Low. Temp. Phys. (to be published) suggest that velocity and frequency dependence should be taken into account. We have used $B=0.89$ in our calculations. This may result in a systematic error in the quoted vortex line densities, but does not influence any of the observations in these experiments.

[26]Model No. 420, Quan-Tech, Boonton, NJ.

[27]For a Gaussian, $\sigma=0.4248\Gamma$, where Γ, is the full width at half maximum.

[28]Donald L. Griswold, Ph.D. thesis, Ohio State University, 1986.

[29]These data were actually taken with $\sigma^2=4$ μW at a 50-Hz bandwidth, which is equivalent to about 0.44 μW below 5 Hz.